A Universal Scale of Apparent Temperature

ROBERT G. STEADMAN

Textile Research Center, Texas Tech University, Lubbock TX 79417

(Manuscript received 29 January 1984, in final form 14 August 1984)

ABSTRACT

Based on the total thermal resistance required by a human model to effect equilibrium, a scale is prepared showing apparent temperature for any combination of dry-bulb temperature, vapor pressure, wind speed and extra radiation likely to be encountered meteorologically. Application to normal midday climates of the United States shows that dry-bulb temperature is modified by the three other variables by from −5 to +7 K. However, multiple linear regression indicates that dry-bulb temperature correlates most strongly with apparent temperature, and provides simple computing formulas.

1. Introduction

A previous work (Steadman, 1971) used the required thermal resistance of apparel to describe windchill at temperatures < 0°C. Subsequently (Steadman 1979a,b), the thermal resistance of the unclothed body was applied to assess sultriness at temperatures > 25°C. The range between 20 and 25°C, in which apparel is needed, was included.

a. Background

The apparent temperature of a set of meteorological conditions T_∞, P_∞, v_{10}, Q_g may be defined as equal to the dry-bulb temperature at $v_{10} = Q_g = 0$, and at a base vapor pressure of moderate humidity, which would require the same thermal resistance, in a walking adult, as this set of conditions.

The previous studies about high and low apparent temperatures left a gap between 0 and 20°C, temperatures which are common outdoors. Since both were based on the common principle of total thermal resistance between the body's core and the meteorological environment, an attempt has been made in this study to meet many requests for an integrated scale of apparent temperature. Moreover, because the empirical and theoretical foundations for the scale are under continual review, the opportunity has been taken to make several modifications, updates and corrections. Since the full background to the earlier scales has already been explained in the aforementioned publications, only the changes are described here. Although improvements will continue to be made as new data appear, especially in the physiological literature, there is a need to summarize existing knowledge and process it into a definitive scale that can provide a precise and versatile means of comparing a variety of weather conditions, whether in reports, forecasts or climatic summaries.

The analysis that follows draws on physiology and textile science at least as much as on meteorology, but the paper is submitted to this journal because meteorologists are more commonly called on to communicate the results to the general public.

b. Scope and limitations

Although the sultriness and windchill scales have found other applications, such as to birds and to mammals other than humans, the present scale is designed and is accurate only for humans, more particularly for healthy adults at moderate activity levels. The work of Saltin and Hermansen (1966) indicates that for such persons the core temperature is limited to 39.5°C, when the person's oxygen consumption reaches its maximum rate. This will be shown to correspond to an apparent temperature of ~54°C. This author cannot guarantee the accuracy of extrapolations which have been made by others to the sultriness scale at apparent temperatures > 54°C. Any results ⩾ 55°C are quoted only for purposes of interpolation and, along with results corresponding to vapor pressures > 4.2 kPa or skin humidities > 90%, are quoted in parentheses. It follows also that a person of average fitness could not sustain the activity level of the present model (178 W m^{-2}) when $T \geqslant 55$°C.

All the world's climatic averages are within the scope of this new scale, but record readings in a few extreme climates are beyond it. Normal apparent temperatures in the sun near 52°C are found in June or July only around the Red Sea, the Persian Gulf, the central Indus Valley and southern Indochina. In the United States, normal July maximum apparent

temperature in the sun near sea level in the southwestern desert is 49°C.

Being based on apparel resistance, this work sheds little light on windchill of the exposed parts of the skin or flesh. The notion of a predetermined skin temperature, such as 33°C, formerly used by some authors, including this one, is superseded by the use of the core temperature as the independent variable. Even calculation of surface temperature from the heat-balance equation for the small part of the skin that is unclothed is not recommended when $\mathcal{T} \leqslant 0$°C, since the erythemal effect of freezing cold has not yet been sufficiently documented to enable precise quantitative treatment.

Apart from the use of "cold" and "hot"—shorthand for conditions referring to the clothed and unclothed model, respectively—the author's policy of not assigning adjectives or forming judgments about comfort or health effects to describe any level of apparent temperature continues. Although many deaths occur due to hypo- and hyperthermia, no attempt is made to describe medical effects of any apparent temperature, since these depend greatly on the time of exposure. The present model refers to continuous, not intermittent, human operation. It derives from the model of Höschele (1970) and includes Höschele's assumption that perspiration evaporates at the skin surface; further cooling due to expansion of this vapor is ignored. This enthalpy correction is important only at very low skin humidities.

c. *Additional criterion for combined index*

A seventh criterion is added to those specified earlier (Steadman, 1979a): If comfort is expressed as a temperature, this should conform to the familiar properties of temperature. Particularly, when all the other parameters are held at their base levels, a given change in dry-bulb temperature should produce an equal change in the index; e.g., a change from $T_\infty = 20$°C, $P_\infty = 1.60$ kPa, $v_{10} = Q_g = 0$ to $T_\infty = 45$°C, $P_\infty = 1.75$ kPa (both at the base vapor pressure and at the same vapor concentration of 12 g m^{-3}) with $v_{10} = Q_g = 0$ translates to a 25°C change in apparent temperature. This is not true of all indices; e.g., the same change affects effective temperature (Yaglou, 1927) by only ~15.5 K, depending on which of several nomograms or computing formulas is used.

d. *Notes on procedure*

The sequence used for assessing any set of meteorological conditions is to determine the resistance (R_f' under "cold" conditions, when $\mathcal{T} \leqslant 25$°C, or R_s under "hot" conditions, when $\mathcal{T} \geqslant 24$°C), as follows:

(i) outdoors, in sun and wind (apparent temperature "in the sun");

(ii) outdoors, in wind, with Q_g set at zero ("shade" apparent temperature);

(iii) with Q_g and v_{10} set at 0 ("indoor" apparent temperature).

Since there is a one-to-one correspondence between thermal resistance and apparent temperature, these resistances are converted into apparent temperatures $\mathcal{T}_{Pvg}$, $\mathcal{T}_{Pv}$, and $\mathcal{T}_P$. The effect of extra radiation is given by $\mathcal{T}_{Pvg} - \mathcal{T}_{Pv}$, the effect of wind by $\mathcal{T}_{Pv} - \mathcal{T}_P$, and the effect of humidity by $\mathcal{T}_P - T_{db}$.

2. Changes to the model

Although the collective effect of the changes seldom alters the apparent temperature by more than 2 K, those separate effects of some magnitude are noted. The first two were made to simplify calculations, particularly to enable the program for an inexpensive programmable calculator to determine all three resistances by iteration in one operation. Copies of programs for HP-34C calculators can be supplied.

a. *Heat generation and loss*

The model's activity, walking at 1.4 m s^{-1}, is taken as generating 177.8, not 180 W m^{-2}, thus making the coefficients of T_∞ and P_∞ integers in the respiration component of heat loss. This becomes $25.7 - 3P_\infty - T_\infty/5$, and the heat loss through the skin $152 + 3P_\infty + T_\infty/5$.

b. *Fabric resistance ratio*

The ratio of moisture-vapor resistance to thermal resistance of a given thickness of moving apparel varies from ~7 K kPa^{-1} in summer clothes to ~11 in winter wear; it is 16.5 in the air gaps. The ratio $Z_f{:}R_f$, previously 0.124, is taken as 1/8.

c. *Scope*

The scale has been enlarged to cover the range of dry-bulb temperatures from −40 to +50°C, as experience in its use suggests reasonable accuracy in very sultry conditions, within the limits of Section 1b.

d. *Base vapor pressure*

Although the base for extra radiation ($Q_g = 0$) has been retained, the vapor-pressure base has been altered slightly to the lesser of (i) $\psi_\infty = 80\%$; (ii) a volume concentration of moisture of 12.0 g m^{-3}. The previous base, $P_\infty = 1.6$ kPa, gave a concentration that declined in inverse proportion to absolute temperature. The new base has a vapor pressure that increases directly with it. (It appears as the zero line in Fig. 2.) It still corresponds to the standard vapor pressure at which textile-testing laboratories in the temperate zone are maintained (X_i in Fig. 2). Another reason for the change is the use of a higher standard in tropical laboratories (X_2 in Fig. 2). The effect is to reduce the

apparent temperature at high dry-bulb temperatures by ~1 K.

e. Base wind speed

The base has been changed to $v_{10} = 0$. This represents a break from traditional values of 5 miles per hour and 2.5 m s^{-1} but, since the model is walking, has the same relative air movement as a wind of 2.7 m s^{-1} at the anemometer on a stationary person. This change shows the full cooling effect of wind, and removes an anomaly in which all but hot winds, with $v_{10} < 2.5$ m s^{-1}, appeared to have a warming effect.

f. Direct solar radiation

The human model, even when walking, is essentially cylindrical, with a maximum projected-area factor of π^{-1}. The computing formula is thus changed to $\phi_3 = 0.380 - 0.0032A$, subject to limits of 0.106 and $\pi^{-1} = 0.318$, reducing ϕ_3 by 0.6 percentage points. This component of extra radiation, often the largest, is given by

$$Q_1 = \phi_3\phi_1 Q_D/\sin A. \quad (1)$$

g. Diffuse incoming sky radiation

This has a vertical component which is more intense than the horizontal component (ASHRAE, 1977, p. 26.26). When the ratio is integrated over all azimuths and applied to the human model, with the above components of π^{-1} (horizontal) and 0.106 (vertical) the average factor, previously taken as π^{-1}, is 0.26, giving the diffuse radiation as

$$Q_2 = Q_d/7. \quad (2)$$

h. Albedo

The reflectance of the earth, following ASHRAE (1977, p. 26.15) is taken as 0.20. The 80% of sunshine absorbed at the surface is accounted for only to the extent that much of it is used to heat air and evaporate moisture from the ground, thus being included in T_∞ and P_∞. The remainder, which may be positive or negative, with a 24-hour average near zero, is reradiated as longwave energy, and is neglected here. Lee (1964) claimed that under extreme conditions reradiation from a desert can add up to 20% to a person's solar heat load.

i. Terrestrial radiation

A previous publication (Steadman, 1979b) was in error in not recognizing that the model is on the surface of a hemisphere with respect to the diffuse reflective power of the Earth. The effect of this and the previous change is to reduce the terrestrial radiation on the model by a factor of $\pi/2$. This part of the extra radiation is given by multiplying the radiation measured on a horizontal actinometer by Earth's reflectivity (0.2), the body's absorptivity (0.7), ϕ_3 and π^{-1}, giving

$$Q_3 = (Q_D + Q_d)/28. \quad (3)$$

j. Incoming extra radiation

Given by the sum of Eqs. 1, 2 and 3, the gross extra radiation sometimes has to be determined at sites where only global radiation is recorded. In these circumstances, an approximation to the sum is

$$Q_1 + Q_2 + Q_3 = (Q_D + Q_d)/6.$$

k. Total extra radiation

Subtraction of outgoing sky radiation from the above sum gives the total extra radiation. The net effect of these changes is to reduce it, typically by one-sixth at midday. Analysis of "full" sunshine (Steadman and Chowdhury, 1985) gives a value of 135 W m^{-2} on an upright walking Caucasian or typically clothed person.

l. Proportion of body's surface clothed

Under "cold" conditions, this is no longer taken as a constant or as a series of steps, since in practice it is a continuum, with more skin being clothed as apparent temperature falls. Common observation in winter indicates that the average person is covered according to

$$\phi_2 = 1 - 0.3 \exp(R'_f/5). \quad (4)$$

This is illustrated in Fig. 1.

m. Correction for wind penetration within apparel

Equation 4 introduces the idea of apparel resistance corrected for the effects of wind and temperature on conductivity, since anything that reduces conductivity requires a compensating extra thickness, which in turn increases the surface area. The effect of wind was previously allowed for phenomenologically and also approximately by adjusting the exponent n in the equation $h_c \propto v^n$ from 0.6 to 0.75. This is too indiscriminate for accurate assessment of windchill. Further analysis of the data (Steadman, 1965), for a clothing ensemble of bulky blanketing covered by taffeta windbreaker cloth, was done. Such an ensemble represents common winter clothing for cold windy conditions, such as parkas or snowmobile suits. As continuous-filament tightly woven taffeta has very low air permeability, the loss of thermal resistance measured must be explained partly by mechanical distortion of the compressible inner fabric and air gaps by wind. Staple-fiber fabrics, such as Byrd cloth (U.S.A.) or ventile fabric (U.K.) approach this level

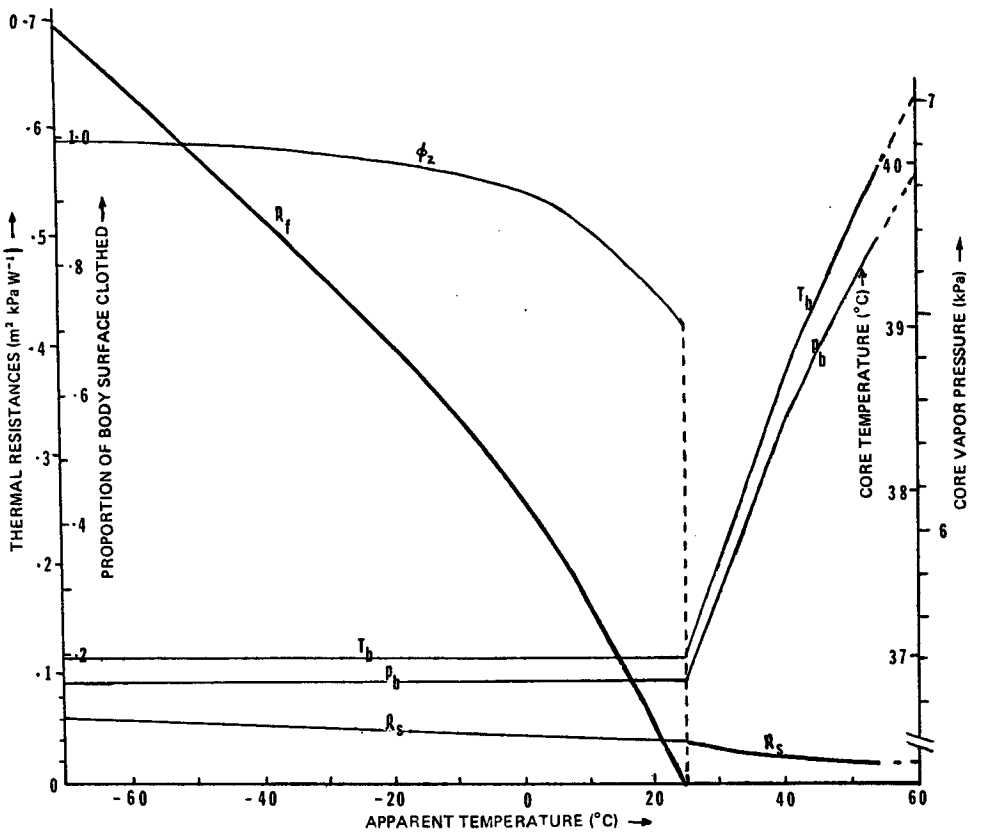

FIG. 1. Model parameters having one-to-one correspondence with apparent temperature.

of impermeability, and are in turn approached by modern microporous materials. But many common winter garments, such as overcoats, natural or synthetic furs with the pile worn on the outside, and garments without hoods or adequate closures, make the wearer more susceptible to windchill than indicated in Table 1.

By subtraction of the surface resistance R_a, this analysis showed that the cooling effect within the fabric is appreciable even at low wind speeds. This has been taken into account to the extent that the apparel is moving, and the loss of thermal resistance is quoted here relative to its value at $v_{10} = 0$. A fit to the limited experimental data gives a ratio

$$\phi_6 = 1/[0.72 + 0.28(h_c/h_{co})^{1/2}] \quad (5)$$

where h_{co} has the value 10.55 W m^{-2} K^{-1}.

Values of ϕ_6 are shown at the top of Table 1.

n. Correction for temperature coefficient of fabric conductivity

The analysis describes a much wider range of temperatures than found in most experiments. Much of the apparel consists of air for which conductivity increases noticeably with temperature. When apparent temperature falls, the logarithmic mean apparel temperature falls by about half as much, giving an effective coefficient of $\sim 1/750$ K^{-1}. Extra radiation also affects conductivity indirectly; the fabric resistance is corrected by a factor

$$\phi_7 = 1 + (T_\infty + R_a Q_g)/750. \quad (6)$$

The factors ϕ_4 and ϕ_5, while used in this work, are not quoted, since they were unchanged from an earlier paper (Steadman, 1979b).

Although the thermal resistance is given by R_f, the thickness of apparel needed is commonly greater than a conductivity of 0.05 W m^{-1} K^{-1} would indicate. Changes in this conductivity due to air temperature, extra radiation and wind are most easily accommodated by Eqs. (5) and (6), which lead to

$$R'_f = \phi_7 R_f \phi_6^{-1}. \quad (7)$$

The program is likewise changed to incorporate Eq. 7 into the calculation of ϕ_2 and R_a, hence R'_f.

o. Surface heat-transfer resistances

The slight distinction between the resistances next to the clothed and unclothed parts of the body has been discontinued since the difference is negligible in comparison with other approximations, such as ignoring variation in R_s over the body. A common

TABLE 1. Effect of wind speed at lower temperatures (windchill).

				v_{10}					
0	2	4	6	8	10	12	15	20	
				h_c					
10.55	11.6	15.0	18.6	22.5	26.3	29.9	35.0	42.7	
				ϕ_6					
1	0.986	0.949	0.916	0.886	0.861	0.839	0.813	0.779	
Temperature (°C)									Humidity increment*
−40	−41.7	−46.7	−50.9	−54.5−	−58.0	−61.0	−64.6	−69.5+	
−35	−36.6	−41.3	−45.3	−48.8	−52.1	−54.9	−58.3	−62.7	−0.1
−30	−31.6	−36.0	−39.8	−43.1	−46.2	−48.8	−52.0	−56.4	
−25	−26.5+	−30.6	−34.2	−37.3	−40.2	−42.7	−45.7	−49.8	−0.2
−20	−21.4	−25.2	−28.6	−31.5−	−34.3	−36.6	−39.3	−43.1	−0.3
−15	−16.2	−19.8	−23.0	−25.7	−28.2	−30.3	−32.8	−36.3	−0.4
−10	−11.1	−14.4	−17.3	−19.8	−22.1	−24.0	−26.3	−29.5+	−0.6
−5	−6.0	−8.9	−11.6	−13.8	−15.8	−17.6	−19.7	−22.6	−0.8
0	−0.9	−3.5−	−5.8	−7.8	−9.6	−11.1	−13.0	−15.5+	−1.2
2	1.1	−1.3	−3.5−	−5.4	−7.1	−8.5−	−10.3	−12.6	−1.3
4	3.2	0.8	−1.2	−3.0	−4.6	−6.0	−7.6	−9.8	−1.5−
6	5.2	3.0	1.1	−0.6	−2.1	−3.4	−4.9	−7.0	−1.6
8	7.3	5.2	3.4	1.8	0.4	−0.8	−2.2	−4.1	−1.8
10	9.3	7.4	5.7	3.2	2.9	1.8	0.4	−1.3	−2.0
12	11.4	9.6	8.0	6.7	5.5−	4.5−	3.3	1.6	−2.2
14	13.4	11.8	10.3	9.0	7.9	7.0	5.9	4.4	−2.4
16	15.4	13.8	12.4	11.2	10.3	9.4	8.4	7.1	−2.6
18	17.4	15.9	14.6	13.5−	12.6	11.9	10.9	9.8	−2.8
20	19.5−	18.0	16.8	15.8	15.0	14.3	13.5+	12.5−	
22	21.5+	20.2	19.0	18.2	17.4	16.8	16.1	15.0	See
24	23.6	22.4	21.4	20.6	19.8	19.3	18.6	17.7	Table
26	25.6	24.6	23.7	23.0	22.3	21.8	21.2	20.5−	3
28	27.7	26.8	26.1	25.5+	25.0	24.7	24.2	23.5−	
30	29.8	29.1	28.6	28.2	2.8	27.6	27.2	26.8	

* Change in apparent temperature due to a humidity change from standard (80% at dry-bulb temperatures ≤ 17.35°C) to zero, when $v_{10} = 0$. At low temperatures, humidity above 80% has negligible effect.

effective diameter, 153 mm, is used to calculate heat transfer coefficients, as derived earlier (Steadman, 1979b).

However, with apparel resistances approaching 0.7 m^2 K W^{-1} at $T = -70$°C, and a typical conductivity, for a moving person, of 0.05 W m^{-1} K^{-1}, an apparel layer as thick as the cylinder's own radius would be required. The convective and evaporative coefficients are proportional to $D^{-0.4}$. Using the relationship between surface area and apparel thickness more generally gives an approximate divisor of $(1 + 0.6R'_f)$ to be applied to the surface resistances, which account for a small part of a well-clad person's total resistance.

These resistances are given by

$$R_a = 1/(1 + 0.6R'_f)(11.4 + 1.86v_{10} + T_\infty/29)$$ when clothed, (8)

$$R_a = 1/(11.6 + 1.86v_{10} + T_\infty/36)$$ when unclothed, (9)

$$Z_a = 1/(128 + 30v_{10})(1 + 0.6\,R'_f)$$ in general. (10)

These linear equations are accurate computing formulas only in the range $3 \leq v_{10} \leq 15$, and were used in preparing the maps. In the computation of tables and charts, the exact values of h_c, shown at the top of Table 1, were used.

p. Core temperature

While apparel is adjusted to maintain a constant core temperature of 37°C in "cold" conditions, part of the body's reaction to "hot" conditions is to become warmer and increase heat loss. The results of Leithead and Lind (1964) indicate an increase in core temperature of 1 K for every 7 K by which equivalent temperature rises above the comfort level or, using the results quoted in Section 1b, 1 K for every $7 \times 25/15.5 \approx 11$ K rise in apparent temperature above the transition temperature of 25°C. This transition temperature (shown in Fig. 2 as a dotted line) represents the boundary between "cold" (clothed) and "hot" (unclothed) conditions. The abrupt change in the model leads to minor anomalies in the results. Applying the relationship between skin resistance and

core temperature derived from the results of Leithead and Lind (1964) we obtain, for hot conditions:

$$T_b = 33.5 + 1/(7R_s). \quad (11)$$

q. Core vapor pressure

As core temperature increases, with $\psi_b = 90\%$, the vapor pressure rises steeply. It is described analogously by

$$P_b = 4.40 + 1/(20R_s). \quad (12)$$

The effects of these two changes are to improve the accuracy of the scale at high apparent temperatures, reducing these by up to 2 K, and to enable the scale to be extended to $T = 55°C$.

r. Skin resistance

Under "cold" conditions, analysis of Fanger's data (1970) indicates that skin tissue reacts to cold by vasoconstriction, raising its resistance approximately according to

$$R_s = 0.040 + R_f/30. \quad (13)$$

That this response is inadequate is shown by the implication that the incremental resistance is 30 times greater in apparel than in skin tissue. Its chief significance is the concomitant rise in Z_s, which greatly reduces heat loss by evaporation.

s. Relationship between skin's resistances to heat and moisture flow

Fanger's (1970) readings, under carefully controlled indoor conditions, showed that the body's various sudomotor mechanisms are five times as sensitive as its vasomotor responses, i.e., $Z_s \propto R_s^5$. In warmer conditions, Kerslake (1972, p. 169), quoting the relationship between sweat rate and skin-tissue conductance as examined by five researchers, presented data which, when processed, lead to an average exponent of 3.1. Such a relationship, if used universally, would indicate sweat rates of the order of 40 W m^{-2} under cold conditions, when $R_s \sim 0.04$. As these are higher than observed, a compromise universal exponent of 4 was used, with

$$Z_s = (12R_s)^4 \quad (14)$$

under all conditions, using the units shown in the Appendix.

3. Determination of apparent-temperature scales

R'_f or Rs was first calculated in one-degree intervals for $-70 \leq T \leq +60°C$ at base levels of P_∞, and with $v_{10} = Q_g = 0$. Values of R'_f provided a reference table which is illustrated, along with R_s for "hot" conditions, as the heavy lines in Fig. 1. By also varying v_{10}, which is arguably the secondary variable under "cold" conditions, values of R'_f were referred to the apparent temperature relationship to assemble Table 1, which also includes the effect of changing humidity.

When the model is exposed to "full" sunshine of 135 W m^{-2} at base levels of humidity, apparent temperature increases by the amounts shown in Table 2. For other values of Q_g, including the negative levels at night and twilight, the effects can be determined accurately by proportion. e.g. If the effect of full sunlight is +6.3 K, the effect of nocturnal radiation of -20 W m^{-2} is $-20 \times 6.3/135 = -0.9$ K.

Tables 3 and 4 show apparent temperature as a function of ambient dry-bulb temperature and relative humidity, with the effect of a wind of 10 m s^{-1} only at base vapor pressure. Table 4 shows extra-radiation effects only at base wind speed.

Tables 1–4 represent a conclusion to the paper. They are believed to be reliable in predicting the magnitude of physiological distress with a single figure, but are subject to future revision. They are based on a wide variety of primary sources. The whole heat-transfer literature lends no support to the notion that windchill should reach a maximum at 25 (Siple and Passel, 1945) or 30 m s^{-1} (Court, 1948), or to the potentially dangerous claim that "wind speeds above 40 miles per hour have little additional chilling effect."

TABLE 2. Increment due to full sunshine.

Dry-bulb temperature (°C)	Wind speed (m s^{-1}) 0	2	4	6	8	10	12	15	20	Humidity increment
−40	7.2	6.8	5.7	4.7	4.0	3.2	3.0	2.9	2.4	0.0
−20	7.4	7.0	5.9	5.0	4.3	3.6	3.4	3.1	2.7	−0.3
0	7.4	7.0	6.0	5.2	4.5	3.8	3.6	3.4	3.0	−1.1
20	8.5	8.3	7.4	6.5	5.5	4.6	4.3	3.8	3.3	See Table
30	8.3	8.1	7.2	6.6	6.2	5.9	5.6	5.3	4.9	4

In the Southern Hemisphere the effect of winter sunshine is 6% lower.

TABLE 3. Effect of humidity at higher temperatures (sultriness).

	ψ_∞											
T_∞	0	10	20	30	40	50	60	70	80	90	100	Wind increment*
20	17.1	17.5−	17.9	18.4	18.8	19.2	19.6	20.0	20.4	20.8	21.2	See
22	19.1	19.6	20.1	20.6	21.1	21.5+	22.0	22.4	22.8	23.2	23.5+	Table
24	21.3	21.9	22.4	22.9	23.3	23.8	24.2	24.6	25.2	25.8	26.4	1
26	23.6	24.2	24.7	25.1	25.6	26.1	26.7	27.3	28.0	28.9	29.8	
28	25.4	25.9	26.5+	27.1	27.8	28.6	29.4	30.4	31.7	32.8	34.3	
30	27.1	27.7	28.4	29.2	30.1	31.1	32.3	33.7	35.3	37.2	(39.6)	
32	28.7	29.5−	30.4	31.4	32.8	34.0	35.7	37.6	40.1	(43.0)		−1.3
34	30.3	31.3	32.5−	33.8	35.0	37.4	39.6	42.7	(46.0)			−0.7
36	31.9	33.1	34.6	35.5+	37.3	40.0	43.0	(48.3)				+0.1
38	33.4	35.0	36.8	39.0	41.8	45.3	(49.7)					+0.6
	0	5	10	15	20	25	30	35	40	45	50	
40	35.0	35.9	36.9	38.0	39.2	40.6	42.0	43.9	45.8	48.2	50.6	+1.1
42	36.6	37.4	38.2	39.6	40.9	42.9	45.0	46.7	48.6			+1.5−
44	38.1	39.4	40.8	42.4	44.4	46.5+	49.0	51.8	(54.1)			+1.8
46	39.7	41.2	43.0	45.0	47.4	50.1	53.3					+1.9
48	41.2	43.1	44.5	46.8	49.6	52.8						+1.9
50	42.8	45.0	47.5−	50.5−	54.0	(58.1)						+1.9

* Change in apparent temperature due to a change in wind speed from 0 to 10 m s^{-1}, at base vapor pressure.

Of interest is the result (Table 4) that the effect of extra radiation is augmented near the upper limits of the scale, especially at high humidity. This has yet to be verified experimentally, but has been reported by people working under conditions where the ambient temperature approximates, and the ambient vapor pressure approaches, that of the unstressed human. The person can reasonably be expected to be more sensitive to extra heat loads when ambient vapor pressure is highest. Since atmospheric vapor also tends to reduce solar intensity, Table 4 and Fig. 4 must be interpreted in the context of full sunshine being less likely at high vapor pressure.

The results are explained and generalized by Figs. 2–4, all of which show the secondary effects as solid, and apparent temperatures as dashed lines. These are drawn on psychrometric charts, which describe conditions to which most people are exposed for at least 99% of their lives, with the constraints $-10 \leq T_\infty \leq 45$°C, $0.1 \leq P_\infty \leq 4.2$ kPa ($-20 \leq T_{dp} \leq 30$°C), $\psi_s \leq 90\%$, $\mathcal{T} \leq 55$°C.

Figure 2 is the basic sultriness chart. The higher sensitivity of apparent temperature at unusually high temperatures and humidities indicates the synergistic effect of these two variables as the body's compensation mechanisms are stressed. The greatest inverse slope of the apparent-temperature isotherms, 5 K kPa^{-1}, is closer to that (zero) of the dry-bulb than the value of 16.5 for the wet-bulb lines, indicating the predominance of dry-bulb temperature in deter-

TABLE 4. Increment due to full sunshine.

	ψ_∞											
T_∞	0	10	20	30	40	50	60	70	80	90	100	Wind increment
20	8.8	8.8	8.8	8.7	8.6	8.6	8.6	8.7	8.8	8.9	9.9	See
30	6.7	7.4	8.0	8.5+	9.0	9.7	10.4	11.1	11.9	12.4	(13.0)	Table 2
	0	5	10	15	20	25	30	35	40			
40	6.4	6.7	7.0	7.4	7.7	8.1	8.7	9.0	(9.4)			−2.1
50	6.3	6.7	(7.2)	(7.8)								−2.0

In the Southern Hemisphere the effect of summer sunshine is 6% higher.

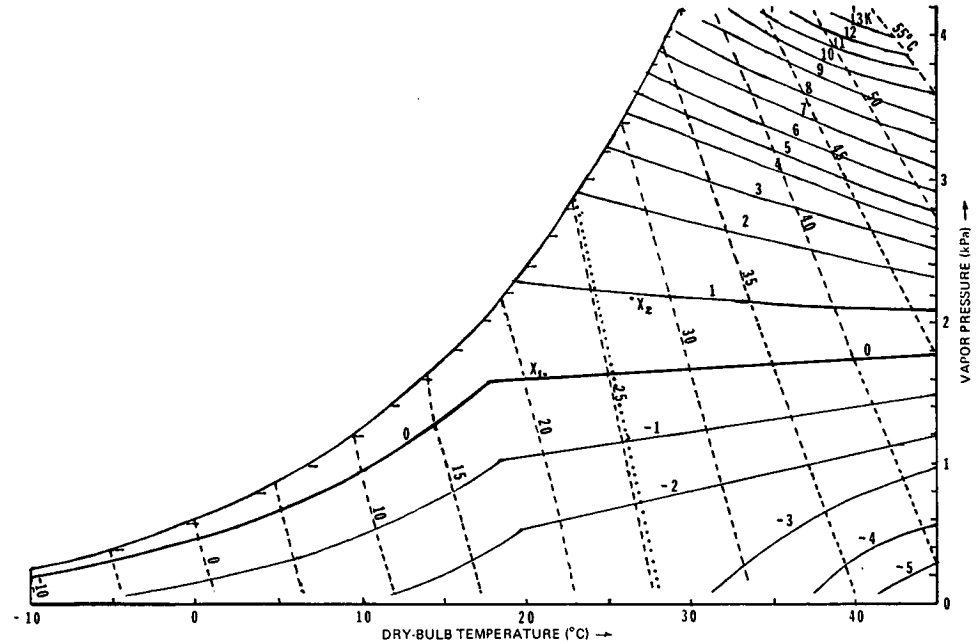

FIG. 2. Vapor-pressure effects (solid lines) and apparent temperatures (dashed lines).

mining heat discomfort. Comfort is often enhanced by evaporative cooling, which is done at constant wet-bulb temperature.

Figure 3 shows the effect of wind on apparent temperature. Windchill increases almost in proportion to $(T_b - T_\infty)$ at low temperatures, but is also appreciable in warm humid conditions, when wind induces evaporation from bare skin. When $T_\infty > T_s$, wind has a net warming effect only when humidity is low. Thus the neutral zone is not a single point, as in effective temperature, but a locus. Tables 3 and 4 and Fig. 3 refer to $v_{10} = 10$ m s^{-1}; as the shape of Fig. 3 changes with wind speed, interpolation and extrapolation to other wind speeds are often inaccurate. Such estimates require the full determination of apparent temperature.

Figure 4 shows the warming effect of "full" sun in calm conditions, which isolate sun effects. Despite

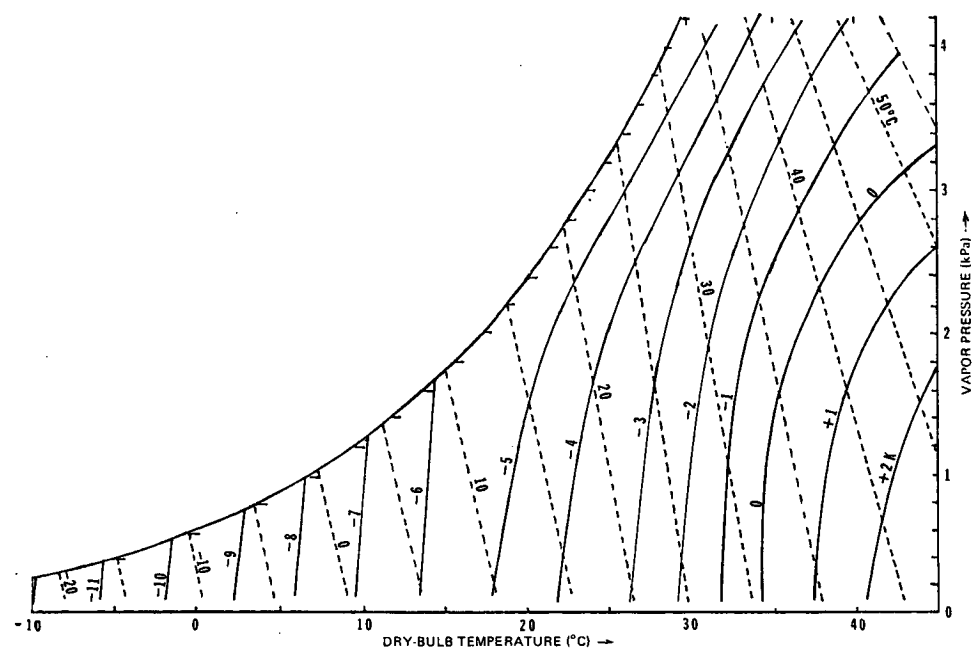

FIG. 3. Wind effects (solid lines) and apparent temperatures in a wind of $v_{10} = 10$ m s^{-1}.

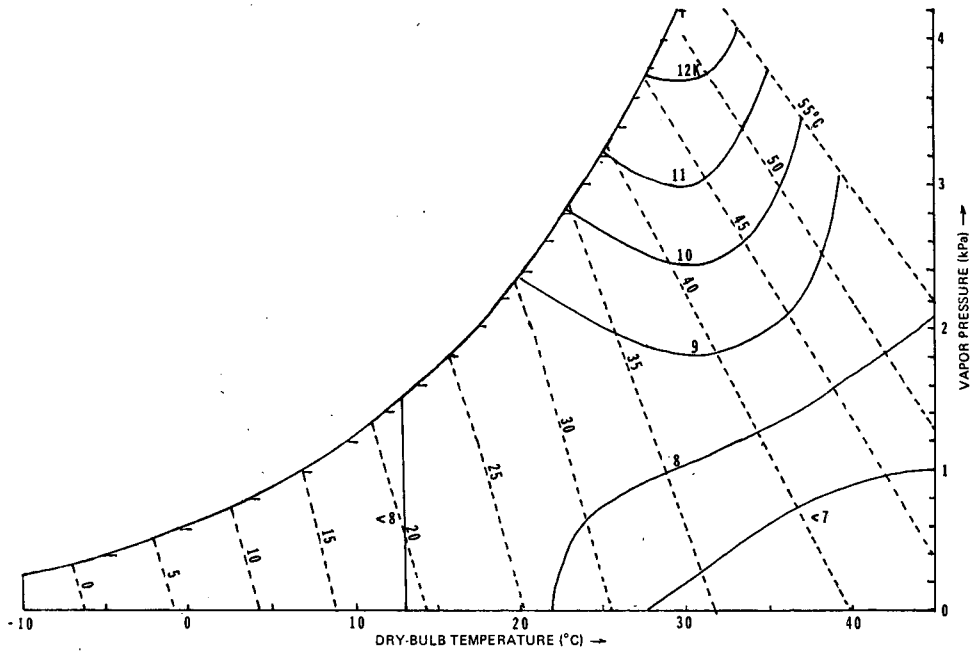

FIG. 4. Extra-radiation effects (solid lines) and apparent temperatures with extra radiation of Q_g = 135 W m^{-2} with v_{10} = 0 m s^{-1}.

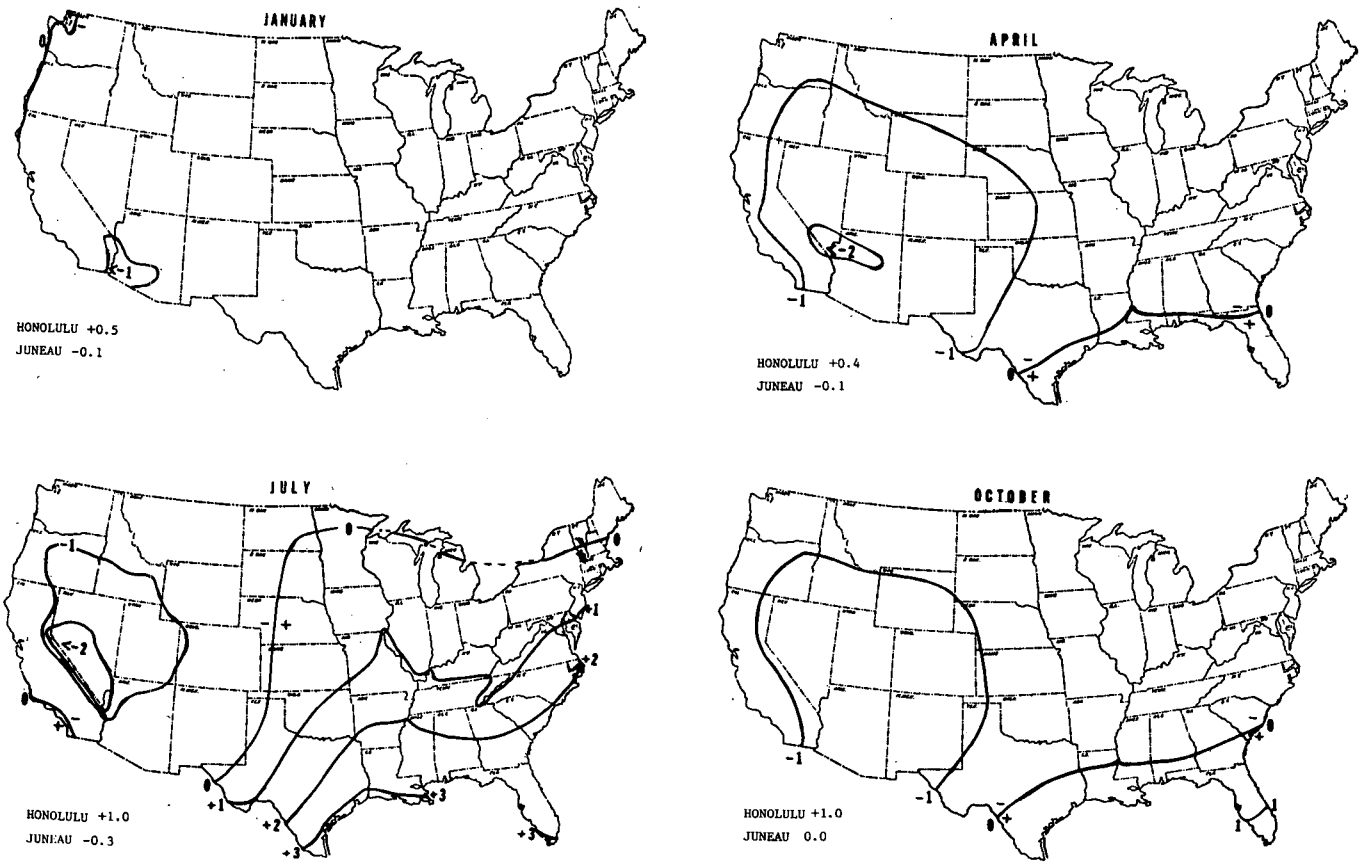

FIG. 5. Seasonal variation in the effect of vapor pressure in normal midday climate.

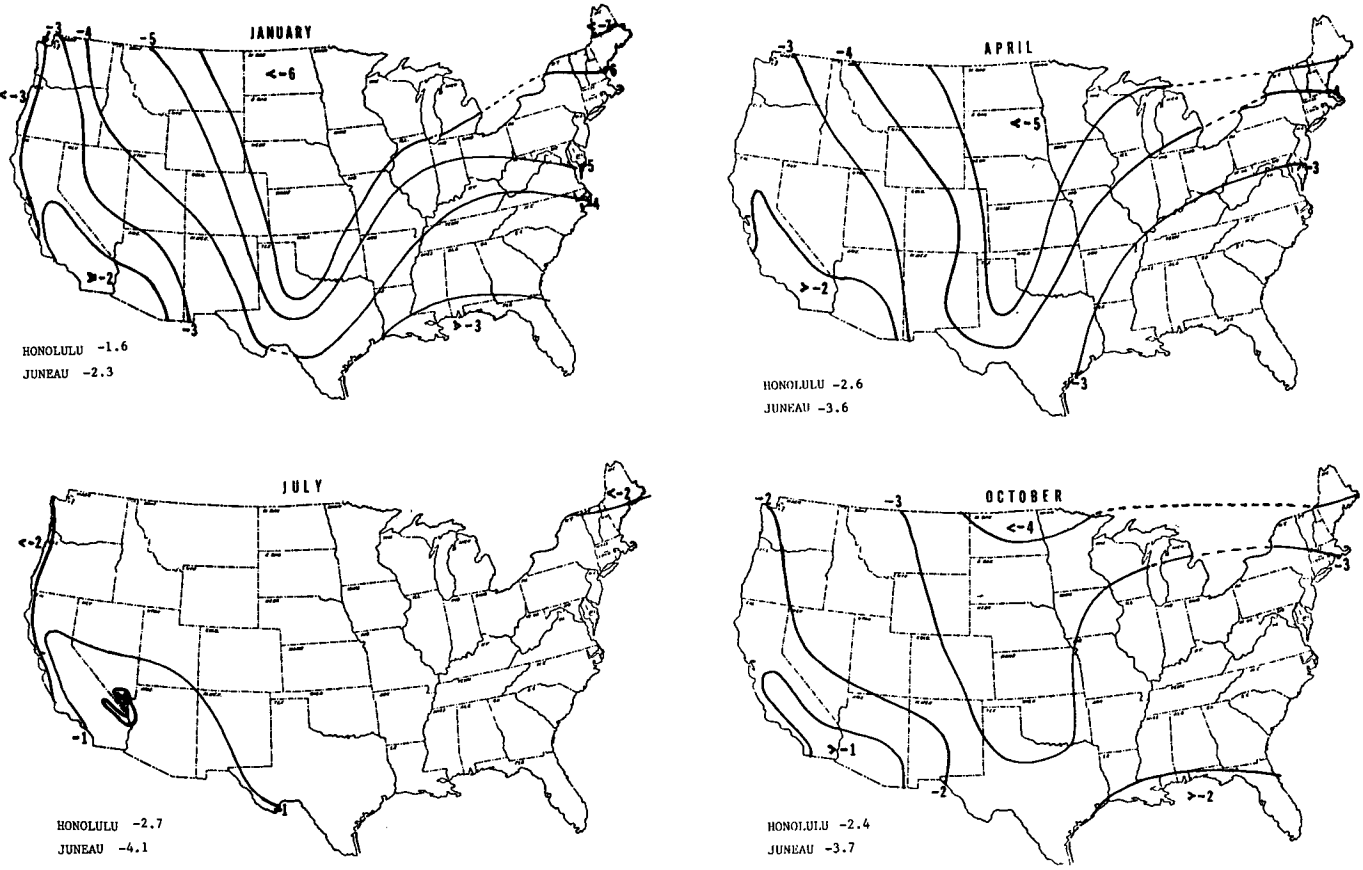

FIG. 6. As in Fig. 5 but of wind.

synergism at high humidities, the model is warmed by ~8 K under ordinary conditions. This effect is little changed by wind speeds < 3 m s^{-1}; at higher speeds, it is multiplied by an approximate factor $10/(7 + v_{10})$ in "cold" and $21/(18 + v_{10})$ in "hot" conditions.

4. Climatological applications

The practice is continued of comparing climates by using midday norms: temperature as $(3T_{max} + T_{min})/4$; vapor pressure derived from the mean dew-point temperature; wind speed as 1.20 times the daily mean, not 1.10, as before. Daily mean insolation on a horizontal surface (Baldwin, 1973) was divided into direct and indirect components using data of the Copper Development Association. These two daily means were converted into noon intensities by latitude-interpolation in the tables of Kusuda and Ishii (1977). Daily mean cloud cover was converted to normal midday values by Landsberg's (1968) factor of 0.85. Other data were obtained from ESSA (1968).

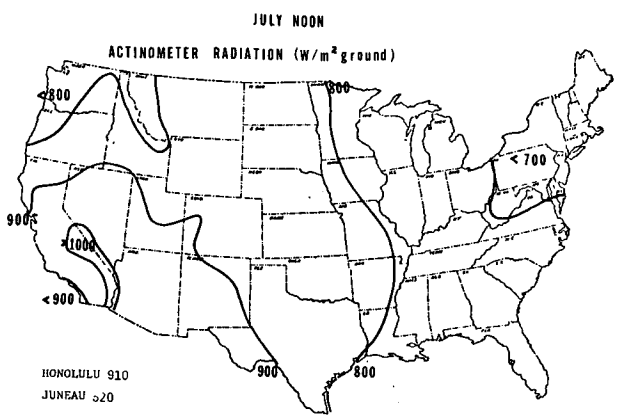

FIG. 7. Normal July noon global radiation.

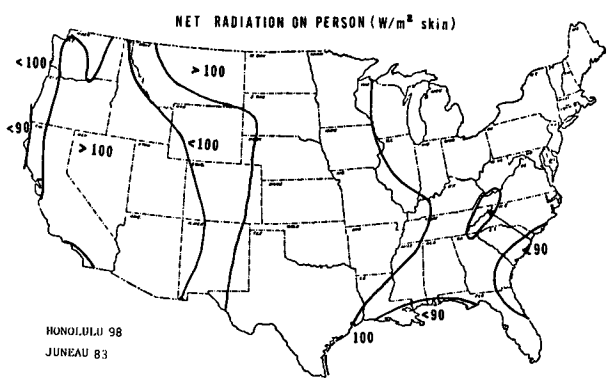

FIG. 8. Normal extra radiation on human, July noon.

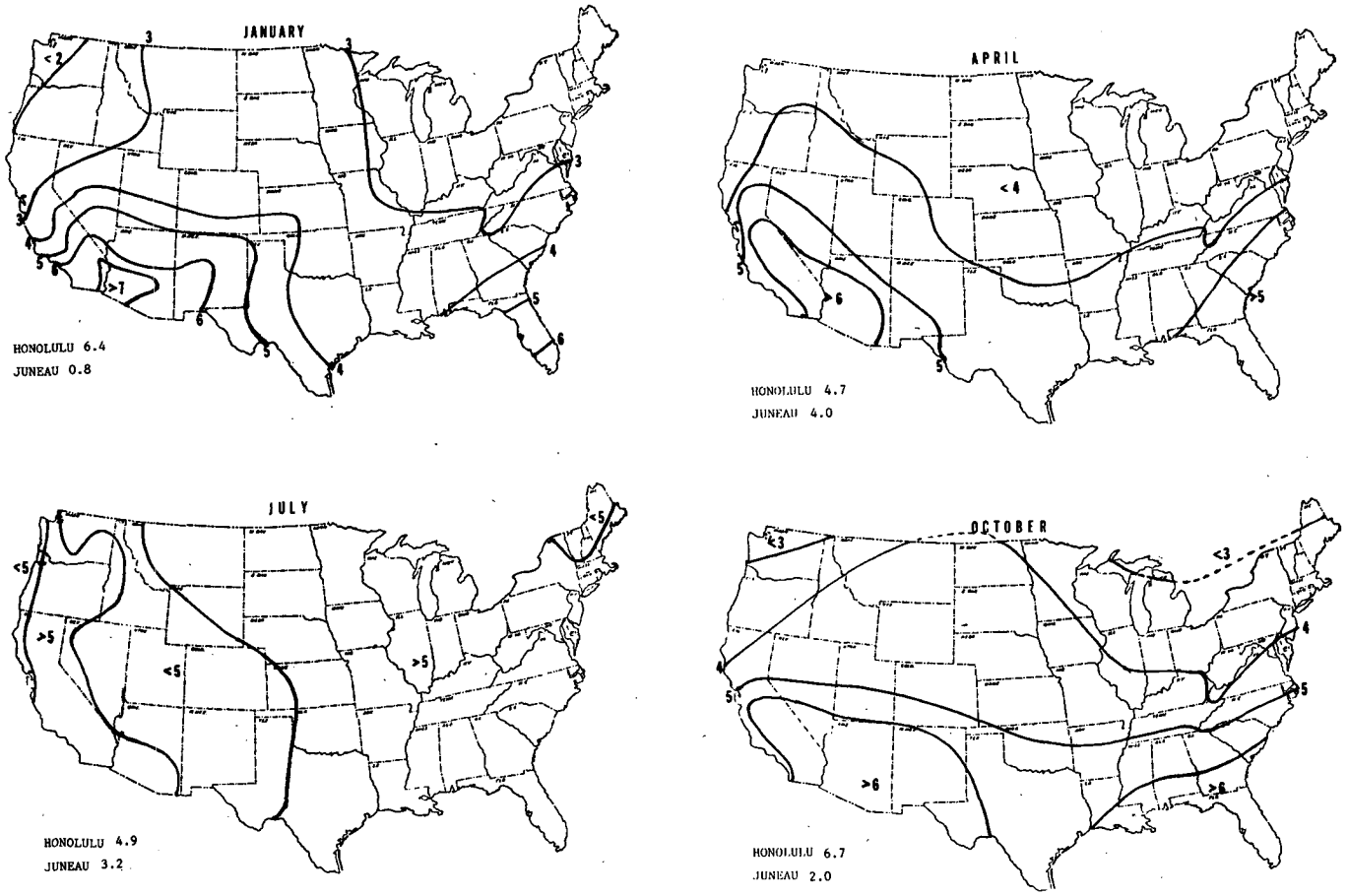

FIG. 9. Seasonal variation in the effect of extra radiation on normal midday conditions.

For months representing the four seasons, the data were processed into T_∞, P_∞, v_{10} and Q_g, thence into the three levels of apparent temperature and the component effects. These effects were not obtained from Tables 1–4, as the increments are exact only at the indicated levels of the other parameters. The effects were determined at 30 stations and mapped.

Figure 5 shows vapor-pressure effects; other maps of dew-point temperature were used to interpolate. Except in summer, the effects are slight. At most temperatures, the zero isopleth corresponds to dew points of 14–15°C. Although normal April temperatures are only slightly below those of October, the effect of vapor pressure is everywhere lower, confirming that the seasonal march of humidity lags behind that of temperature, which in turn follows seasonal variation in day length by about a month. For the same reason, January and July maps also approximately represent humidity effects, and even apparent temperatures, of February and August respectively.

Figure 6 charts windchill. The cooling effect of wind is expectedly greater in winter, showing the effect of cold in the north and wind speed in the central plains. Of interest is a small part of the southwestern desert in July, which shows the rare warming effect of hot dry wind. Summer sea breezes on the Gulf and Atlantic coasts cool by evaporation.

Using July sunshine as an example, Figs. 7 and 8 illustrate the derivation of Fig. 9. Figure 7 shows July noon global radiation, derived from Baldwin (1973). It may be contrasted with the calculated Q_g values in Fig. 8. In desert and mountain areas, the latter tend to be lower than Fig. 7 would suggest, because they take account of appreciable extra radiation to the sky through clear dry air. Direct sunshine on the upright human tends to be higher at noon at high latitudes, where the solar altitude is lower.

When extra radiation is expressed as a warming effect (Fig. 9), the shape of the isotherms is again different, because synergism between humidity and solar warming tends to be greatest in the southeast where July sunshine is least intense. The result is an almost uniform solar warming across the conterminous states in normal July noon conditions. April results are similar to those of October (Fig. 9), the more intense sunshine of April being offset by the lower solar altitude and higher humidity in October.

Figure 10 combines the effects of Figs. 5, 6 and 9. It is also a measure of the amount by which dry-bulb temperature overestimates (−) or underestimates (+)

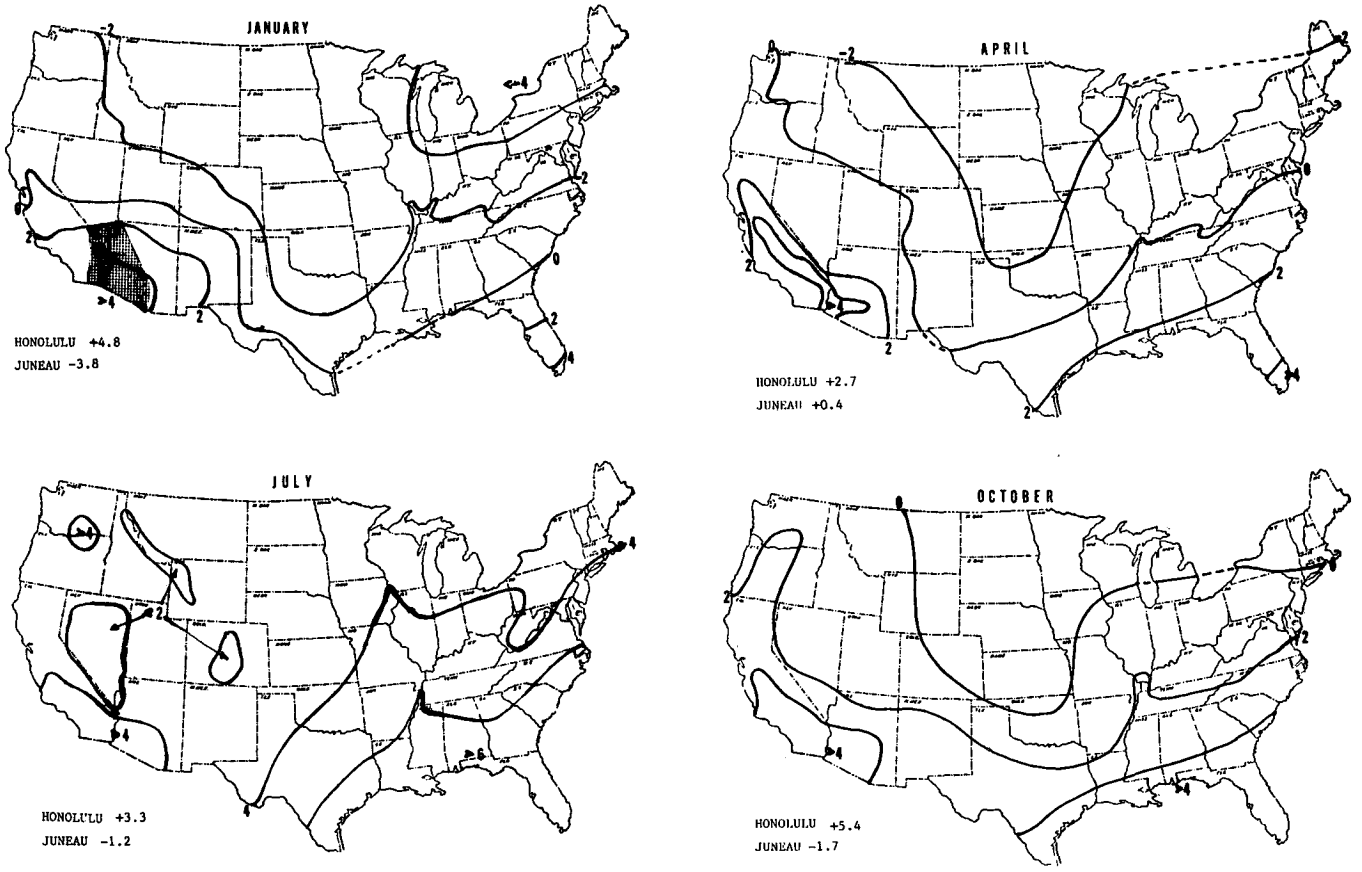

FIG. 10. Seasonal variation in the combined effects of vapor pressure, wind and extra radiation, normal midday condition.

the temperature as sensed by a walking person outdoors near noon. In January, only Florida and the far southwest show enough warming from the sun to offset wind and dryness effects by a degree or more. Also noticeable is the scant northward progress made by this combined effect between January and April. The shaded area shows the only part of the conterminous states where this total warming effect is greater in January than in July.

Figure 11 shows, approximately in mountain areas, the outdoor apparent temperature "in the sun." Interpolation uses the result (Steadman and Chowdhury, 1985) that apparent temperature has a lapse rate of ~8.2 K km^{-1}. Despite the considerable attention paid to humidity, those places having the highest apparent temperatures are also those with the highest dry-bulb temperatures; the partial correlation coefficient for 120 pairs of results is 0.991, compared with 0.779 between apparent temperature and vapor pressure. This is consistent with correlations in Australia (Steadman, 1983) and the Indian subcontinent (Steadman and Chowdhury, 1985). Further work, in which these results are combined with a method of rapidly determining degree days (Steadman, 1978), is in progress, with the aim of estimating heating, cooling and dehumidifying needs in terms of apparent temperature.

5. Simplified formulas for determining apparent temperatures

Because of interest expressed in avoiding the tedium of determining apparent temperatures by the method outlined in this publication and its forerunners, the three sets of 120 $\mathcal{T}$ values obtained underwent four multiple regression analyses:

(i) for indoor apparent temperature $\mathcal{T}_P$;

(ii) for shade apparent temperature $\mathcal{T}_{Pv}$;

(iii) for apparent temperature in the sun $\mathcal{T}_{Pvg}$, when the actinometer readings Q_D and Q_d are used without the need to calculate Q_g; this was analyzed with all likely meteorological variables, including ϕ_4, ϕ_5, altitude, monthly rainfall and latitude. The last four fell short of statistical significance at the 5% level;

(iv) for $\mathcal{T}_{Pvg}$, based on calculated Q_g.

As the number of parameters needed in the regression increases, so too does the uncertainty in estimating apparent temperature by this short method. Results are in Table 5, with each regression equation

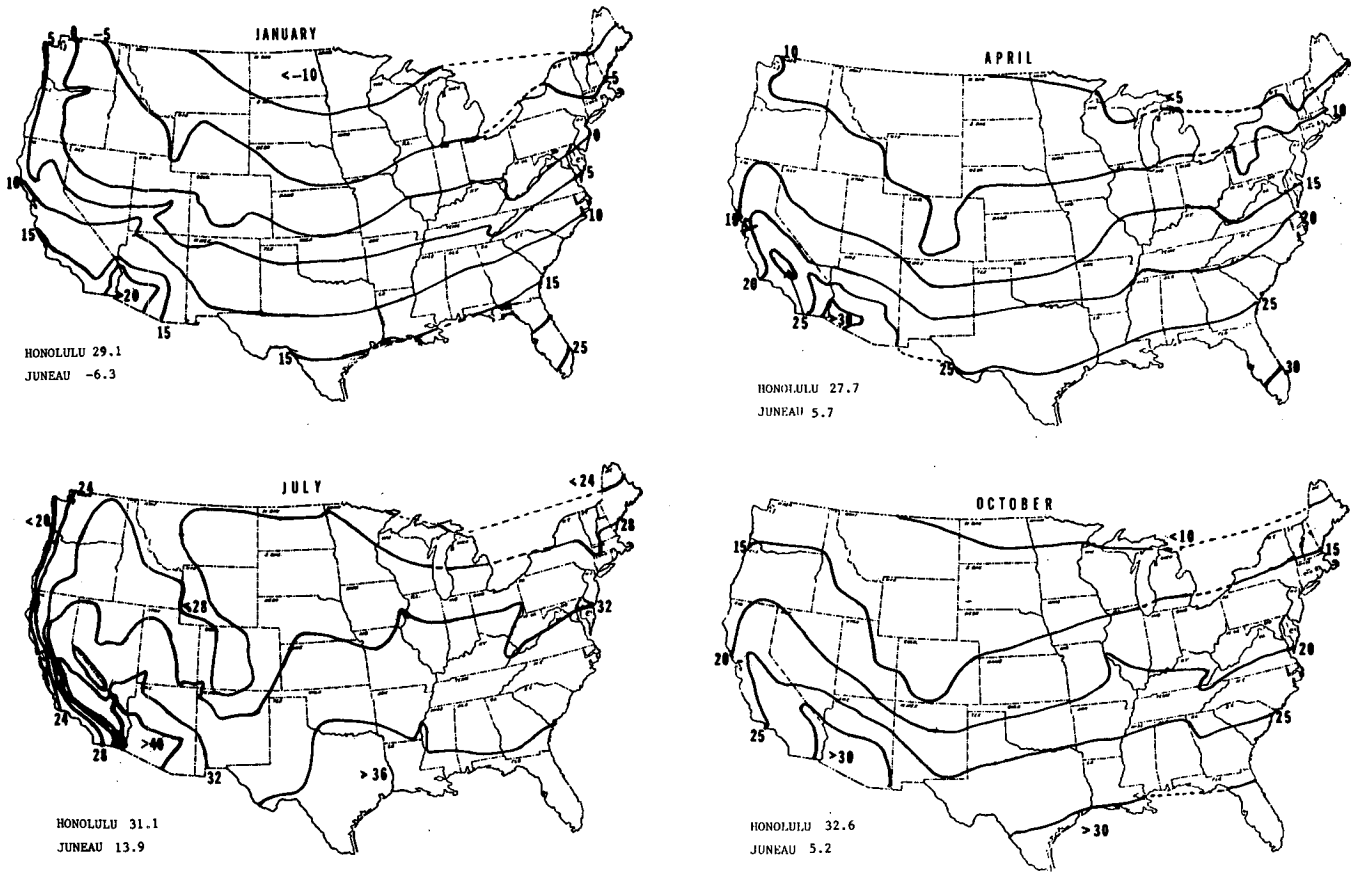

FIG. 11. Seasonal variation in normal midday apparent temperature in sunlight.

followed by the residual standard deviation and with the parameters shown in order of importance. Under each term is the percentage of total variation explained by the parameter.

TABLE 5. Linear regression equations for apparent temperature.

Conditions	Equation	Residual standard deviation (K)
Indoors	$\mathcal{T}_P = -1.3 + 0.92T_\infty + 2.2P_\infty$ 99.6% 0.3%	0.32
Shade	$\mathcal{T}_{Pv} = -2.7 + 1.04T_\infty + 2.0P_\infty - 0.65v_{10}$ 98.9% 0.5% 0.5%	0.44
Sun; actinometer readings	$\mathcal{T}_{Pvg} = 4.5 + 1.02T_\infty - 1.00v_{10}$ 98.3% 0.7% $+ 2.8P_\infty - 5.8\phi_5 + 0.0054(Q_D + Q_d)$ 0.4% 0.3% 0.04%	0.54
Sun; Q_g derived	$\mathcal{T}_{Pvg} = -1.8 + 1.07T_\infty + 2.4P_\infty$ 98.3% 0.7% $- 0.92v_{10} + 0.044Q_g$ 0.4% 0.4%	0.51

Essentially similar formulas have been obtained using 25 stations in Australia in July and January, despite generally different levels of all the variables. The greater residual error in estimating $\mathcal{T}_{Pvg}$ using actinometer readings is the price paid for the convenience of avoiding calculation of the person's extra radiation.

Intervals for 95% confidence are of the order of ± 1 K even near the variables' central values (in the United States at midday $T_\infty = 17°C$, $P_\infty = 1.09$ kPa, $v_{10} = 4.18$ m s^{-1}, $Q_g = 94$ W m^{-2}). Use of such formulas adds to whatever random variance and systematic error are inherent in the theory. Their scope is further limited by their being based only on midday data.

Acknowledgments. Thanks are due to the National Climatic Center, Asheville, NC, for performing the multiple-regression analyses and providing a grant toward publication costs.

APPENDIX

Symbols

A solar altitude angle (deg)
P vapor pressure (kPa)

Q	heat-transfer rate per unit area of body surface; exception: Q_D and Q_d refer to unit area of horizontal surface (W m^{-2})
R	resistance to heat transfer of unit area (m^2 K W^{-1})
R'_f	resistance of unit area of apparel on moving person, corrected for variations in conductivity relative to that at $T_\infty = v_{10} = 0$
T	temperature
Z	resistance of unit area to moisture transfer (m^2 kPa W^{-1})
v_{10}	wind speed measured by anemometer 10 m above ground and averaged over 1 min
$\mathcal{T}$	apparent temperature; with P, v, g as subscripts, only the indicated combination of humidity, wind and extra radiation applies
ϕ_1	ratio of effective radiating area to total surface area
ϕ_2	proportion of body surface covered by apparel
ϕ_3	ratio of body's projected area to effective radiating area
ϕ_4	fraction of sky covered by cloud
ϕ_5	fraction of solar radiation, on horizontal surface, that is direct
ϕ_6	ratio of apparel resistance at given wind speed to value at $v_{10} = 0$
ϕ_7	ratio of apparel conductance at given level of T_∞ and Q_g to value when $T_\infty = Q_g = 0$
ψ	relative humidity (%)
Subscripts	
a	boundary layer of air
b	body core
D and d	direct and diffuse insolation on horizontal surface
db	dry bulb
dp	dew point
g	net extra radiation per unit area of body surface
max	maximum
min	minimum
s	skin tissue; at surface of skin
∞	ambient

REFERENCES

American Society of Heating, Refrigerating and Air-Conditioning Engineers, 1977: *Handbook of Fundamentals,* New York, ASHRAE, ~800 pp.

Baldwin, J., 1973: *Climates of the United States.* NOAA, Washington DC, 113 pp.

Copper Development Association, no date: Solar energy systems. New York, CDA, 42–48.

Court, A., 1948: Windchill. *Bull. Amer. Meteor. Soc.,* **29,** 487–493.

Environmental Science Services Administration, 1968: *Climatic Atlas of the United States,* Washington DC, 80 pp.

Fanger, P. O., 1970: *Thermal comfort.* Danish Technical Press, 244 pp.

Höschele, K., 1970: Ein Modell zur Bestimmung des Einflusses der klimatischen Befinden des Menschen. *Arch. Meteor. Geophys. Bioklim.,* **B18,** 83–99.

Kusuda, T., and Ishii, T., 1977: *Hourly Solar Radiation Data for Vertical and Horizontal Surfaces on Average Days in the United States and Canada.* Natal. Bur. Stand., Washington DC, 405 pp.

Landsberg, H.E., 1968: *Physical Climatology,* 2nd ed. Gray, DuBois PA, 446 pp.

Kerslake, D. McK., 1972: *The Stress of Hot Environments.* Cambridge University Press, 316 pp.

Lee, D. H. K., 1964: Terrestrial animals in dry heat: Man in the desert. *Handbook of Physiology,* Sect. 4, D. B. Hill, Ed. Washington DC, Amer. Physiol. Soc., 551–582.

Leithead, C. S., and A. R. Lind, 1964: *Heat Stress and Heat Disorders.* London, Churchill (quoted in Kerslake, p. 129).

Saltin, B., and Hermonsen, 1966: Esophageal, rectal and muscle temperature during exercise. *J. Appl. Physiol.,* **21,** 1760.

Siple, P. A., and C. F. Passel, 1945: Measurements of dry atmospheric cooling in subfreezing temperatures. *Proc. Amer. Phil. Soc.,* **89,** 177–199.

Steadman, R. G., 1965: Simultaneous heat and moisture transfer through clothing textiles in the presence of wind. Ph.D. thesis, University of New South Wales, 202 pp.

——, 1971: Indices of windchill of clothed persons. *J. Appl. Meteor.,* **10,** 674–683.

——, 1978: The determination and metrication of degree days. *ASHRAE J.,* **20,** 38.

——, 1979a: The assessment of sultriness. Part 1: A temperature-humidity index based on human physiology and clothing science. *J. Appl. Meteor.,* **18,** 861–873.

——, 1979b: The assessment of sultriness. Part 2: Effects of wind, extra radiation and barometric pressure on apparent temperature. *J. Appl. Meteor,* **18,** 874–885.

——, 1983: Unpublished videotaped lecture to Bureau of Meteorology, Melbourne.

——, and A. Chowdhury, 1985: Sultriness in the Indian subcontinent. *Indian J. Meteor.,* (in press).

Yaglou, C. P., 1927: Temperature, humidity and air movement in industries: The effective temperature index. *J. Ind. Hyg.,* **9,** 297–309.